Available online at www.sciencedirect.com
SCIENCE DIRECT®
Physics Letters B 591 (2004) 55–60
PHYSICS LETTERS B
www.elsevier.com/locate/physletb

The influence of $\nu h_{11/2}$ occupancy on the magnetic moments of collective 2_1^+ states in $A \sim 100$ fission fragments

A.G. Smith [a], D. Patel [a], G.S. Simpson [a,1], R.M. Wall [a], J.F. Smith [a], O.J. Onakanmi [a], I. Ahmad [b], J.P. Greene [b], M.P. Carpenter [b], T. Lauritsen [b], C.J. Lister [b], R.V.F. Janssens [b], F.G. Kondev [b,2], D. Seweryniak [b], B.J.P. Gall [c], O. Dorvaux [c], B. Roux [c]

[a] *University of Manchester, M13 9PL, Manchester, UK*
[b] *Physics Division, Argonne National Laboratory, Argonne, IL 60439, USA*
[c] *Institut de Recherches Subatomique, CNRS-IN2P3, et Université Louis Pasteur, 67037, Strasbourg, France*

Received 26 January 2004; accepted 24 March 2004

Available online 12 May 2004

Editor: V. Metag

Abstract

The magnetic moments of $I^\pi = 2_1^+$ states in even–even $A \sim 100$ fission fragments have been measured using the Gammasphere array, using the technique of time-integral perturbed angular correlations. The data are interpreted within the context of the interacting boson model (IBA2) leading to the suggestion of a strong $\nu h_{11/2}$ component in the deformed 2_1^+ states of this region.

The $A \sim 100$ region of neutron-rich nuclei is an ideal subset of the nuclear chart in which to investigate the origins of nuclear collectivity. One sees near $N = 50$, nuclei characteristic of the shell model. If neutron number is increased, a transition to deformed rotational behaviour is observed at $N \approx 60$. This transition is particularly sharp in the case of $_{38}$Sr and $_{40}$Zr but becomes steadily weaker as Z is increased. A useful indicator of this transition is the ratio of the excitation energies of the lowest $I^\pi = 4^+$ and 2^+ states. In the case of Zr, $E_{4_1^+}/E_{2_1^+}$ is 1.6 for $N = 58$, 2.6 for $N = 60$, and approaches the rotational limit ($3\frac{1}{3}$) with a value of 3.1 for ^{102}Zr. In contrast, $E_{4_1^+}/E_{2_1^+}$ varies slowly in the isotopes of $_{46}$Pd, from a value of 2.2 in ^{102}Pd to 2.58 in ^{116}Pd. The onset of rotational collectivity is also observed in the large reduced transition probabilities ($B(\mathrm{E2}; 2 \to 0)$ values) shown in Table 1.

Talmi [1], Federman and Pittel [2,3] and Casten [4] have all stressed the importance of neutron–proton interactions in producing deformed states in this region of the nuclear chart. Specifically, the proton $g_{9/2}$, and the neutron $g_{7/2}$ and $h_{11/2}$ orbitals are thought to be most important in establishing collectivity [2,3]. Casten [4] has shown that $E_{4_1^+}/E_{2_1^+}$

E-mail address: gavin.smith@man.ac.uk (A.G. Smith).
[1] Present address: ILL, Grenoble, France.
[2] Present address: Nuclear Engineering Division, ANL, Argonne, USA.

0370-2693
doi:10.1016/j.physletb.2004.03.091

Table 1
g factors of 2^+ states in the $A \sim 100$ region. The γ-ray pairs which define the angular correlation are given in the form $E_i \otimes E_j$ where E_i and E_j are the γ-ray energies (in keV) of the populating and depopulating transitions, respectively. For each pair several isotropic gates are used to ensure clean selection of the nucleus of interest. B(E2) values for the $2_1^+ \rightarrow 0_1^+$ transitions have been calculated from the lifetimes with corrections made for internal conversion

Nucleus	E_{4^+}/E_{2^+}	ϕ_p (mrad)	τ (ns)	B(E2) ($e^2\,b^2$)	B (Tesla)	g	Correlations used
^{98}Zr	1.51	+1(38)	< 0.29 [31]		−27.4(4)		621 ⊗ 1223, 648 ⊗ 1223
^{100}Zr	2.65	+301(24)	0.78(3) [32,33]	0.22(1)	from [40]	+0.30(3)	352 ⊗ 213, 497 ⊗ 213
^{102}Zr	3.14	+810(150)	2.76(36) [34,35]	0.32(4)		+0.22(5)	326 ⊗ 152, 487 ⊗ 152
^{102}Mo	2.51	+92(44)	0.180(6) [36]	0.20(1)	−25.6(1)	+0.4(2)	584 ⊗ 297
^{104}Mo	2.92	+340(20)	1.040(59) [36]	0.28(2)	from [41]	+0.27(2)	368 ⊗ 192, 519 ⊗ 192
^{106}Mo	3.03	+460(40)	1.803(43) [34]	0.28(1)		+0.21(2)	351 ⊗ 172, 511 ⊗ 172
^{108}Mo	2.91	+420(130)	0.72(43) [37]	0.4(2)		+0.5(3)	371 ⊗ 193
^{106}Ru	2.64	+170(80)	0.29(3)[a]		−47.8(1)	+0.3(1)	445 ⊗ 270, 581 ⊗ 270
^{108}Ru	2.74	+265(34)	0.498(43) [34]	0.19(2)	from [42]	+0.23(4)	423 ⊗ 242, 575 ⊗ 423
^{110}Ru	2.75	+430(60)	0.433(29) [35]	0.23(2)		+0.44(7)	423 ⊗ 241, 576 ⊗ 241
^{112}Ru	2.73	+470(90)	0.462(43) [34,38]	0.23(2)		+0.44(9)	408 ⊗ 237, 545 ⊗ 237
^{110}Pd	2.46	+47(31)	0.067(2) [39]	0.16(1)	−42(2)	+0.3(2)	547 ⊗ 374, 653 ⊗ 374
^{114}Pd	2.56	+55(26)	0.289(87) [38]	0.07(2)	from [43]	+0.09(5)	520 ⊗ 332, 648 ⊗ 332
^{116}Pd	2.58	+67(27)	0.159(43) [25]	0.11(3)		+0.2(1)	538 ⊗ 341, 682 ⊗ 341

[a] Lifetime estimated assuming same transition quadrupole moment as ^{108}Ru.

varies reasonably smoothly with the product of the number of active neutrons (neutron holes) N_n, with the number of active protons (proton holes) N_p. In obtaining a smooth curve, it is necessary to count protons from the $Z = 38$ shell gap if $N < 60$ but from $Z = 28$ if $N \geqslant 60$. The closure of the gap at $Z = 38$ is possibly a result of the interaction between the $\pi g_{9/2}$ and the $\nu g_{7/2}$ spin–orbit partners. The importance of the occupation of $\nu h_{11/2}$ intruder orbitals is stressed in the shell-corrected rotating liquid-drop calculations of Skalski et al. [5]. At intermediate spin, the low-Ω components of the $\nu h_{11/2}$ orbital are often identified with the S bands in the even–even nuclei of this region, and there is experimental evidence for rotational bands built on this orbital in odd-neutron Sr, Zr, Mo, Ru and Pd nuclei [6–14]. It should be pointed out, however, that the experimental evidence for the influence of the $\nu h_{11/2}$ on deformation is based mainly on level structures and branching ratios at spins greater than $I = 2$, interpreted within the context of rotational models.

To better determine the influence of the $h_{11/2}$ orbital on structural change in this region, it is crucial to have other experimental observables that allow direct access to the details of the wavefunction of the 2_1^+ state. In particular, given that the neutron–proton interaction is suspected as the driving force behind the establishment of collectivity, the g factor has particular relevance. While determination of the electric quadrupole moment can give important information on the deformation of the nucleus, it is the g factor with its very different sensitivity to the neutron and proton degrees of freedom that allows neutron and proton contributions to the collectivity to be disentangled. From a theoretical point of view, g factors of deformed nuclei should be investigated at a fundamental level through a shell-model representation of the collective state using a suitable basis and residual interactions, but the basis space required to contain the physics of the whole region turns out to be extremely large, allowing only restricted shell-model calculations. On the other hand, it is possible to include the effect of shell gaps through the use of the interacting boson model (IBA2) [15]. In the limit of good F-spin, this model gives the collective g factor as

$$g_R = g_\pi \frac{N_\pi}{N_\pi + N_\nu} + g_\nu \frac{N_\nu}{N_\pi + N_\nu},$$

where N_π and N_ν are the number of proton and neutron bosons (or boson holes), respectively, and g_π and g_ν are the proton– and neutron–boson g factors, respectively. This expression is useful because it can

be used in transitional regions of the nuclear chart, as long as one knows the particle numbers associated with the dominant shell closures. Naturally, if all shell gaps are ignored, and the boson g-factors are taken to be $g_\pi = 1$ and $g_\nu = 0$, the IBA2 expression yields $g_R = Z/A$, the value expected for collective motion of a uniformly charged droplet. The underlying microscopic basis of the IBA2 approach is expressed in the variation of g_π with Z and g_ν with N.

The $A \sim 100$ region of deformed rotors is most readily accessed using spontaneous fission. The development of high-efficiency, high granularity Ge-detector arrays such as Euroball [16] and Gammasphere [17] has allowed many neutron-rich nuclei to be investigated through the use of ^{252}Cf and ^{248}Cm fission sources. Recently, a technique has been developed that allows access to the g-factors of states with lifetimes of the order of a nanosecond [18]. This technique uses the 4π geometry of Gammasphere and Euroball to measure the time-integral perturbed angular correlations (IPAC) of secondary-fragment γ rays emitted following implantation into a ferromagnetic host. In this Letter, we present the g-factors of the 2_1^+ states in 13 neutron-rich even–even nuclei and interpret the data in terms of the IBA2 model with effective neutron– and proton–boson g factors.

The data presented here are based on an experiment performed using the Gammasphere array at the Argonne National Laboratory, USA. A ^{252}Cf source of approximately 100 μCi total activity was sandwiched between two 15 mg cm^{-2} Fe foils. The Fe–Cf–Fe sandwich was placed at the centre of the Gammasphere array of 101 Compton-suppressed Ge detectors. A pair of small permanent magnets provided a field of 0.2 T in the plane of the foil and in the direction normally reserved for the beam to Gammasphere. The direction of the applied field was reversed once every eight hours by rotating the magnet assembly through 180°. The experiment was run for two weeks, during which time 9.95×10^9 events of three or more γ rays were detected.

Fission fragments from ^{252}Cf stop in the Fe foil within a few picoseconds of the fission event. For states with lifetimes much longer than this stopping time, γ-ray decay may be considered as occurring from a nucleus implanted within the Fe lattice and the transient magnetic fields that are experienced while the fragment moves through the lattice may be safely ignored. At the implantation site the nucleus of the fission fragment experiences an impurity hyperfine magnetic field that is constant in time and whose magnitude and sign depend on the atomic number of the fission fragment. Impurity hyperfine magnetic fields are typically of the order of a few tens of tesla and are sufficient to cause a significant Larmor precession in the 2_1^+ states of the majority of fission fragments. For a static field B the average precession angle ϕ_p of a state with mean lifetime τ is given by

$$\phi_p = -\frac{\mu_N g B \tau}{\hbar},$$

where g is the g-factor of the state and μ_N is the nuclear magneton. The Larmor precession of the nuclear spin vector generally affects the distribution of magnetic substates and the precession angle may therefore be determined from a careful measurement of angular correlations between γ rays that populate and depopulate the state of interest. In all the cases discussed here, both populating and depopulating γ rays are of electric quadrupole (E2) type. Details of the analysis procedure and the Gammasphere geometry may be found in Ref. [18]. Determination of the g factor from the measured precession requires knowledge of the average static field at the implantation site, which may be substitutional or interstitial. Care is required in using tabulated measurements of impurity hyperfine fields since annealed sources yield a higher fraction of nuclei at substitutional sites than is the case when radioactive ions are simply implanted into the ferromagnetic host. For this reason we have ensured that the average field is consistent with implantation measurements in the case of the Zr and Mo isotopes, and in the case of Ru and Pd where the average field is lower in implantation measurements we have used only implantation data.

Table 1 gives the results of the precession measurements. In all cases, triple γ-ray coincidences have been used to cleanly select the nucleus of interest and in most cases the angular correlation has been measured between the $4_1^+ \to 2_1^+$ and $2_1^+ \to 0^+$ transitions as well as between the $6_1^+ \to 4_1^+$ and $2_1^+ \to 0^+$ transitions. For all the nuclei in this study, the lifetime of the 4_1^+ state is much shorter than that of the 2^+, and the measured value of $\phi_p(2_1^+)$ as determined using the $6_1^+ \to 4_1^+ \otimes 2_1^+ \to 0^+$ correlation can easily be corrected using an independent measurement of $\phi_p(4_1^+)$. The third γ ray in each event is used as

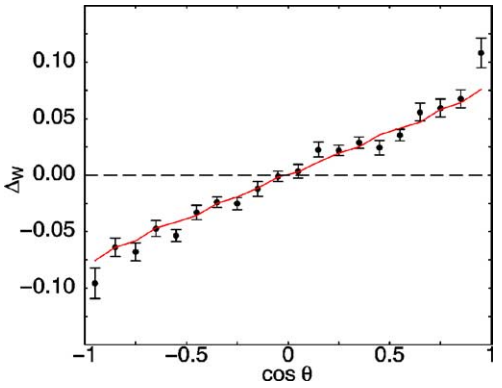

Fig. 1. The perturbation to the angular correlation function Δ_W for the $4_1^+ \to 2_1^+ \otimes 2_1^+ \to 0^+$ coincidence in ^{106}Mo. The solid line shows a projection of a fit to the data. The data are plotted as a function of $\cos\theta$, where θ is the angle between the detection axes of the γ rays. For an unperturbed angular correlation, Δ_W is zero for all values of $\cos\theta$.

an *isotropic gate* [18] (i.e., the energy is specified but not the direction) to improve selectivity. A combination of isotropic gates, each generating a clean final spectrum, is used for each measurement. As an example, the data for ^{106}Mo are presented in Fig. 1 which shows the quantity Δ_W, determined from the experimental data and approximately equal to the product of ϕ_p and the logarithmic derivative of W for small values of ϕ_p [18].

The results of this work are presented in Fig. 2 together with data from previous g factor measurements in $^{102-110}$Pd [19], ^{100}Zr [20,21], ^{98,100}Mo [22], ^{102,104}Mo [23], ^{98,104}Ru [24], ^{102}Ru [25] and ^{100,102}Ru [26]. Where there is an overlap between this and other work, i.e., in the cases of ^{100}Zr and ^{102,104}Mo, there is excellent agreement which provides supporting evidence for the validity of the technique and the saturation of the impurity hyperfine fields. In general, the g factors obtained in this work lie below Z/A indicating that uniform rotation/vibration of a uniformly charged drop is not a valid picture for the collective states of this region. The sudden change in the structure of the 2_1^+ states in the Zr isotopes that occurs at $N = 58$ results in a change from the negative g factors of ^{92,94}Zr [27] to near zero for ^{96}Zr [28] and then to positive values for ^{100,102}Zr. In the Mo and Ru isotopes, where the onset of deformation is more gradual, the g factors show a pronounced decrease from values close to Z/A for $N \leqslant 60$ to a minimum of around 0.2 at $N = 64$. The data suggest that the decrease in the 2_1^+ state g factor also occurs in the Pd isotopes, though, as with the onset of deformation, the effect occurs at higher neutron numbers than in the case of Mo and Ru.

The large variation in the g factors with neutron number suggests that it may be possible to gain some insight into the neutron orbitals that are involved in driving deformation in this region. In an attempt to separate neutron and proton degrees of freedom, we have carried out calculations within the IBA2 scheme with different values of g_π and g_ν. In these calculations we have taken the number of proton and neutron bosons according to the prescription of Casten [4], i.e., by counting proton bosons from the $Z = 28, 50$ shell closures for $N > 60$ and for $N = 60$ by using effective proton–boson numbers to reproduce the energy systematics. This allows us to work within a framework in which the E_{4^+}/E_{2^+} ratio depends smoothly on the product $N_\pi N_\nu$. We count neutron bosons between the $N = 50$ and $N = 82$ shell closures. Fig. 2 shows the results of three such calculations with the following parameters: $g_\pi = 1.0$, $g_\nu = 0.05$; $g_\pi = 0.65$, $g_\nu = 0.05$; $g_\pi = 1.0$, $g_\nu = -0.1$. Sambataro and Dieperink [29] have shown that with $g_\pi > 1.0$ and $g_\nu \approx 0$ it is possible to reproduce the g factors of the Ru and Pd nuclei with $N \leqslant 60$ and the Pd nuclei with $N \leqslant 64$. It is clear from our calculations that this choice of parameters yields results that are too large to explain the most deformed nuclei in this data set, ^{100,102}Zr and ^{104,106}Mo, while giving rough agreement with ^{110,112}Ru. Far better agreement with most of the nuclei measured in this work is obtained if either g_π is reduced to around 0.65, or if g_ν is made slightly negative. Since to a first approximation, g_π should be a function of proton number only, it is preferable to suppose that the marked variation of the g factors with neutron number is a result of a small change in g_ν rather than to a larger variation in g_π. Furthermore, a choice of $g_\pi \approx 1$ and $g_\nu \approx 0$ gives consistency with IBA2 fits to data in other regions of the nuclear chart, notably the rare-earth nuclei discussed in Ref. [30]. In the simple picture of collective orbital motion $g_\nu = 0$; a shift to negative values may be taken as an indication of the filling of single-particle orbitals that couple to give a 2^+ state with a negative g factor.

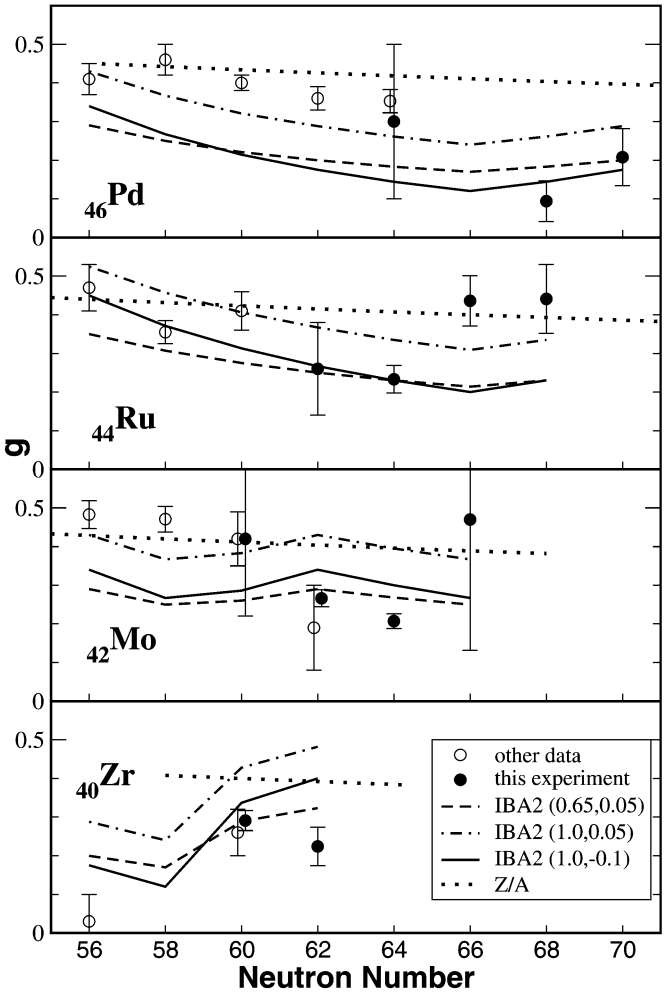

Fig. 2. Summary of the g factor measurements of 2_1^+ states in the $A \sim 100$ region from this, and other work. The experimental results are compared with the predictions of the IBA2 model using values of (g_π, g_ν) given in the legend.

According to the deformed shell-model calculations of Skalski et al. [5], the neutron Fermi level for the nuclei presented here should lie in the region of the $g_{7/2}$, $d_{3/2}$ and $h_{11/2}$ orbitals. Of these, only $h_{11/2}$ couples to give a 2^+ state with a negative g factor; for a pure $\nu g_{7/2}^2$, $L = 2$ configuration $g = +0.42$, while $g(\nu h_{11/2}^2,\ L = 2) = -0.35$. These considerations lead to the suggestion that the large deformations in this region are associated with the filling of low-Ω $h_{11/2}$ neutron orbitals, rather than $\nu g_{7/2}$ orbitals. In the Pd nuclei, the decrease may be delayed because there is a lower proton contribution to the collectivity, leading to the nucleus having lower deformation and a smaller $h_{11/2}$ component for a given neutron number. To determine more precisely the contribution of $h_{11/2}$ orbitals to the g factors of the 2_1^+ states would require a large-basis shell-model calculation using appropriate residual interactions and is beyond the scope of this work.

In conclusion, the g factors of the 2_1^+ states in 13 neutron-rich fission fragments have been determined using the recently developed application of IPAC to fission-fragment spectroscopy. This has lead to a significant extension in the known g-factor data of this region of the nuclear chart. The interpretation of these data within the framework of the IBA2, with neutron– and proton–boson numbers constrained by

the variation in the energies of the first 2^+ and 4^+ states with $N_\pi N_\nu$, has lead to the conclusion that the onset of deformation is associated with an increasing contribution of a neutron orbital which couples to give a 2^+ state with a negative g factor. It is suggested that the filling of low-Ω $h_{11/2}$ orbitals is likely to be responsible.

Acknowledgements

This project was supported by the UK EPSRC and the US Department of Energy (contract No. W-31-109-ENG-38). The authors are indebted for the use of the ^{252}Cf to the Office of Basic Energy Sciences, US Department of Energy, through the transplutonium element production facilities at the Oak Ridge National Laboratory.

References

[1] I. Talmi, in: F. Iachello (Ed.), Interacting Bosons in Nuclei, Plenum, New York, 1979, p. 79.
[2] P. Federman, S. Pittel, Phys. Lett. B 69 (1977) 385;
P. Federman, S. Pittel, Phys. Lett. B 77 (1978) 29;
P. Federman, S. Pittel, Phys. Rev. C 20 (1979) 820.
[3] P. Federman, S. Pittel, R. Campos, Phys. Lett. B 82 (1979) 9.
[4] R.F. Casten, Phys. Lett. B 152 (1985) 145.
[5] J. Skalski, S. Mizutori, W. Nazarewicz, Nucl. Phys. A 617 (1997) 282.
[6] M.A.C. Hotchkis, et al., Nucl. Phys. A 533 (1991) 111.
[7] I. Ahmad, W.R. Phillips, Rep. Prog. Phys. 58 (1995) 1415.
[8] W. Urban, et al., Nucl. Phys. A 689 (2001) 605.
[9] K. Butler-Moore, et al., Phys. Rev. C 52 (1995) 1339.
[10] S.J. Zhu, et al., Phys. Rev. C 65 (2002) 014307.
[11] Z. Zhang, et al., Phys. Rev. C 67 (2003) 064307.
[12] J.K. Hwang, et al., Phys. Rev. C 56 (1997) 1344.
[13] X.Q. Zhang, et al., Phys. Rev. C 61 (1999) 014305.
[14] R. Krücken, et al., Phys. Rev. C 60 (1999) 031302.
[15] A. Arima, et al., Phys. Lett. B 66 (1977) 205;
T. Otsuka, et al., Phys. Lett. B 76 (1978) 139.
[16] P.J. Nolan, F.A. Beck, D.B. Fossan, Annu. Rev. Nucl. Part. Sci. 45 (1994) 561.
[17] I.Y. Lee, Nucl. Phys. A 520 (1990) 641c.
[18] D. Patel, et al., J. Phys. G 28 (2002) 649.
[19] J.M. Brennan, M. Haas, N.K.B. Shu, N. Benczer-Koller, Phys. Rev. C 21 (1980) 574.
[20] A. Wolf, et al., Phys. Rev. C 40 (1989) 932.
[21] K. Wolke, et al., Z. Phys. A 334 (1989) 491.
[22] P.F. Mantica, et al., Phys. Rev. C 63 (2001) 034312.
[23] G. Menzen, et al., Z. Phys. A 321 (1985) 593.
[24] G.K. Hubler, H.W. Kugel, D.E. Murnick, Phys. Rev. C 9 (1974) 1954.
[25] K. Johansson, et al., Nucl. Phys. A 188 (1972) 600.
[26] K. Auerbach, K. Siepe, J. Wittkemper, H.J. Körner, Phys. Lett. 23 (1966) 367.
[27] G. Jakob, et al., Phys. Lett. B 468 (1999) 13.
[28] G. Kumbartzki, et al., Phys. Lett. B 562 (2003) 193.
[29] M. Sambataro, A.E.L. Dieperink, Phys. Lett. B 107 (1981) 249.
[30] M. Sambataro, et al., Nucl. Phys. A 423 (1984) 333.
[31] K. Kawade, et al., Z. Phys. A 304 (1982) 293.
[32] A.G. Smith, et al., J. Phys. G 28 (2002) 2307.
[33] B. Singh, Nucl. Data Sheets 81 (1997) 1.
[34] R.C. Jared, H. Nifenecker, S.G. Thompson, LBL-2366, 38 (1974).
[35] E. Cheifetz, et al., in: Proc. Conf. Nucl. Spectroscopy of Fission Products, Grenoble, France, 1979, p. 193.
[36] M. Liang, et al., Z. Phys. A 340 (1991) 223.
[37] H. Penttiläa, et al., Phys. Rev. C 54 (1996) 2760.
[38] R.C. Jared, H. Nifenecker, S.G. Thompson, in: Proc. 3rd Symp. Phys. Chem. of Fission, New York, 1973, vol. 2, Int. At. Energy Agency, Vienna, 1974, p. 211.
[39] L.E. Svensson, PhD thesis, Uppsala University, 1989.
[40] A.R. Arends, F. Pleiter, Hyperfine Interact. 7 (1979) 361.
[41] P. Bond, S. Jha, Phys. Rev. C 2 (1970) 1887;
R.H. Dean, G.A. Jakins, J. Phys. F 8 (1978) 1563;
M. Kontani, J. Itoh, J. Phys. Soc. Jpn. 22 (1967) 345.
[42] G.F. Koster, Nuclear Chemistry Annual Report, Lawrence Berkeley Laboratory, USA, 1970.
[43] A. Alzner, et al., Z. Phys. A 302 (1981) 223.